RSC Advances

PAPER

View Article Online
View Journal | View Issue

Cite this: *RSC Adv.*, 2025, **15**, 2632

Advancing bio-filter materials for enhanced desalination in agricultural applications†

K. K. T. Thilanka,[a] R. H. W. Pathinayaka,[a] W. P. V. S. Udayanga,[a] Rohini M. de Silva *[ab] and K. M. Nalin de Silva *[a]

The global scarcity of irrigation-grade water poses severe concerns in the agricultural sector. Desalination techniques including reverse osmosis, electrodialysis, capacitive deionization, membrane filtration, and multi-stage flash are some dynamic solutions to mitigate this challenge. In this study, novel bio-filter materials were explored and developed for the application of membrane-based electrodialysis. Firstly, a series of composites were synthesized comprising different compositions of carboxymethyl cellulose (CMC), graphene oxide (GO), and *Aloe vera* to serve as cationic-selective membranes. Then desalination abilities of the composite series were assessed through permselectivity and ion exchange capacity (IEC) studies. Membrane matrix developed by integrating all the above three materials exhibited the highest permselectivity and IEC. The composites were characterized using Fourier Transform Infrared Spectroscopy (FT-IR), Scanning Electron Microscopy (SEM) and X-ray diffraction (XRD). It was determined that the designed composites can function effectively as cationic-selective membranes, while dried banana leaves can serve directly as an anionic-exchanger in an electrodialysis apparatus. Optimal performance was achieved when the pH of the system was maintained between 4.5 and 8.1. This system successfully desalinated a 3.5% (w/v) sodium chloride solution, achieving ~75% desalination within 20 minutes. The potential to use banana leaves as a bio-filter material was explored in a parallel study. The results revealed that banana leaves dried for over 28 days at room temperature have high potential to function as anionic-selective membranes effectively in the electrodialysis desalination process. Altogether, this innovative approach offers a sustainable, eco-friendly and cost-effective solution for electrodialysis based water desalination.

Received 21st October 2024
Accepted 19th January 2025

DOI: 10.1039/d4ra07538b

rsc.li/rsc-advances

1. Introduction

Despite water covering most of the Earth's surface, the world is currently facing an escalating water scarcity crisis due to insufficient access to potable and freshwater resources. Alarming statistics show that over two billion people struggle with water shortages, while the agricultural sector accounts for more than 70% of global water withdrawals.[1] As a result, securing adequate water resources for crop cultivation has become an increasing challenge, particularly as the global population continues to rise and the demand for food escalates. Desalination techniques, which purify seawater and brackish water, present a promising solution to address these challenges.

Traditional desalination technologies, such as reverse osmosis (RO) and multi-stage flash distillation, are widely used but face significant challenges. These methods are energy-intensive, expensive, and often rely on fossil fuels, contributing to environmental concerns. The high operational pressures and maintenance costs associated with RO further limit its feasibility, particularly in resource-constrained settings. Electrodialysis (ED), on the other hand, presents a promising alternative due to its lower energy consumption, operational simplicity, and potential for energy optimization. ED operates by applying a voltage across ion-exchange membranes to selectively separate ions dissolved in water.[2–5] ED already addressed many of the limitations associated with traditional desalination technologies. Ion-selective membranes are essential for efficient electrodialysis (ED), but traditional and commercially available synthetic membranes, often derived from petrochemicals are costly, associated with high a ecological footprint, and require complex manufacturing processes.[6,7] Innovative solutions are needed to balance high desalination efficiency with reduced preparation costs and minimized environmental impact, ensuring the broader applicability of ED in addressing global water scarcity.[8,9]

To address the challenges associated with existing synthetic membranes, biofilter materials are being explored as

[a]*Centre for Advanced Materials and Devices (CAMD), Department of Chemistry, Faculty of Science, University of Colombo, Colombo, Sri Lanka. E-mail: kmnd@chem.cmb.ac.lk; rohini@chem.cmb.ac.lk*

[b]*Department of Life Sciences, Faculty of Science, NSBM Green University, Pitipana, Homagama, Sri Lanka*

† Electronic supplementary information (ESI) available. See DOI: https://doi.org/10.1039/d4ra07538b

sustainable alternatives. This study explores novel bio-filter materials, including Carboxymethyl Cellulose (CMC), Graphene Oxide (GO), *Aloe vera*, and dried banana leaves, as sustainable alternatives to synthetic membranes.

In this study bio-based cation selective membrane membranes are composed of carboxymethyl cellulose (CMC), graphene oxide (GO), and *Aloe vera* extract, combining to offer an eco-friendly, cost effective and efficient alternative to traditional synthetic membranes. CMC, a biocompatible polymer with intrinsic cation-exchange properties, serves as the structural framework for the membrane matrix.[10] The carboxylate ($-COO^-$) groups in CMC create a high-density negative charge, which attracts cations such as Na^+ and Mg^{2+} while repelling anions like Cl^- and SO_4^{2-}. The hydroxyl (–OH) groups in its cellulose backbone further enhance the hydrophilicity of the membrane, facilitating water uptake and creating hydration layers that support efficient ion transport.[11,12]

The incorporation of GO and *Aloe vera* extract into the CMC matrix improves the membrane's properties. GO, a functionalized derivative of graphene, enhances the negative charge density and forms strong electrostatic interactions with cations, which improves ion selectivity.[13,14] Additionally, GO provides excellent mechanical reinforcement to the polymer matrix, enhancing the structural integrity of the membrane. The oxygen-containing functional groups of GO can interact *via* strong hydrogen bonding with CMC and electrostatic interactions with charged species, allowing for tunable surface chemistry that enables the development of a more robust and selective membrane.[15,16] *Aloe vera* extract, rich in polysaccharides and hydrophilic compounds, increases the negative charge density and supports water retention, further enhancing ion transport and hydration. *Aloe vera* also contains bioactive ingredients like acemannan and anthraquinones, which have natural antimicrobial properties, helping to reduce biofouling in membranes and increase their lifetime and efficiency during water treatment processes.[17–20] These materials further improve the mechanical strength, conductivity, and thermal stability of the membranes, making them suitable for the demanding operational conditions of the ED process.[15,17]

In addition to cation-selective membranes, the study also explores the use of bio-based anion-selective membranes. These membranes typically rely on cationic functional groups in the matrix to facilitate anion selectivity. In this study, dried banana leaves (*Musa* spp.) were investigated as natural ion-exchange membranes.[21–23] Despite limited prior research on banana leaves for membrane applications, studies have highlighted their natural ability to regulate ions such as sodium (Na^+) and chloride (Cl^-), suggesting inherent selective permeability.[24] Experimental analyses in our study revealed that banana leaves dried for more than 21 days exhibited optimal permselectivity with significantly high anion exchange capacity. Consequently, banana leaves dried for 28 days were utilized as anion-selective membranes in the ED desalination process.

The objective of this study is to develop and evaluate bio-based membranes for sustainable desalination. Specifically, it aims to (i) synthesize and characterize cation-selective membranes incorporating CMC, GO, and *Aloe vera* extract, (ii) assess their permselectivity and ion-exchange capacity, (iii) explore dried banana leaves as anion-selective membranes, and (iv) establish an electrodialysis apparatus to test the desalination efficiency of these bio-filter materials.

The significance of this study lies in its demonstration that biofilter materials can achieve higher ion removal rates (desalination efficiency) compared to systems using commercially available synthetic membranes.[25,26] It also revealed that the ion exchange capacity of the cation-selective membrane exceeds that of some commercial membranes, positioning it within the commercial range.[8] Furthermore, this study uniquely utilized dried banana leaves as anion-selective membranes for desalination without any chemical pretreatment, relying solely on a 28 day drying process, highlighting a sustainable, cost-effective and novel approach.

2. Experimental and methods

2.1 Synthesis of carboxymethyl cellulose polymer

CMC (5.00 g, low viscosity, Sigma-Aldrich) was added to 100 mL of water heated to 80 °C and stirred until fully dissolved. Citric acid (1.20 g, assay 99%, HiMedia Laboratories Pvt. Ltd) and glycerol (3.80 g, assay 99.5%, SRL) were then added while stirring and maintaining the above temperature. The solution was then heated up to 100 °C, while stirring for 30 min. Subsequently, the temperature was raised to 120–130 °C and maintained with continuous stirring for 1 h. The polymer solution was poured into Petri dishes and oven-dried at 60 °C for 24 h.

2.2 Synthesis of graphene oxide

Graphite powder (3.00 g, Bogala vein graphite) was mixed with 100 mL of 98% sulfuric acid (Qualikems Lifesciences Pvt. Ltd) and stirred at 97 °C for 2 h. The mixture was cooled to 15–20 °C, and potassium permanganate (15.00 g, assay 99.5%, Techno Pharmchem, India) was added slowly over 1 h. The solution was stirred for 30 min, then heated to 97 °C. Cooled distilled water (150 mL) was added dropwise over 30 min, followed by 500 mL of distilled water and 15 mL of 30% hydrogen peroxide (Breckland, UK), resulting in a yellowish-gold solution. The solution was filtered, washed twice with 10% HCl (assay 35.0%, DAEJUNG Chemicals & Metals Co., Ltd) and distilled water, and centrifuged at 3000 rpm for 30 min. The final GO stock solution was added into Petri dishes dried at 80 °C for 2 h.

2.3 Synthesis of carboxymethyl cellulose/*Aloe vera* polymer

Aloe vera gel (15.00 g, Wadula gardens, Piliyandala, Sri Lanka) extracted and was blended into a solution. Then, a portion (10.00 mL) of this blended solution was mixed with distilled water (90.00 mL) and heated to 80 °C. CMC (5.00 g) was introduced to this solution instead of 100 mL of water at 80 °C as described in the previous step of synthesis of CMC polymer, and the identical procedure was followed afterwards.

2.4 Synthesis of carboxymethyl cellulose/GO polymer

Graphene oxide (130.00 mg) was dissolved in distilled water (250.00 mL) and stirred for 2 hours, followed by sonication for

90 min. Afterwards, the solution was stirred for 1 h. A portion (40.00 mL) of this solution was mixed with distilled water (60.00 mL). The mixture was stirred for 15 min, and the temperature was increased to 80 °C. CMC (5.00 g) was added to the mixture and stirred until fully dissolved. Then, citric acid (1.20 g) and glycerol (3.8 g) were added while stirring. The temperature was then raised to 100 °C and maintained for 30 min with continuous stirring. Subsequently, the temperature was increased to 120–130 °C and stirred for 1 h. The final solution was poured into Petri dishes and oven-dried at 60 °C for 16 h.

2.5 Synthesis of carboxymethyl cellulose/GO/*Aloe vera* composite

Graphene oxide (130.00 mg) was dissolved in distilled water (250.00 mL) and stirred for 2 h, followed by sonication for 90 min. Afterwards, the solution was stirred for 1 h. A portion (40.00 mL) of this solution was then mixed with blended *Aloe vera* gel solution (10.00 mL) and distilled water (50.00 mL). Again, it was stirred for 1 h and the temperature of the mixture was increased up to 80 °C. CMC (5.00 g) was introduced to the mixture and stirred until completely dissolved. Citric acid (1.20 g) and glycerol (3.8 g) were added while stirring. The temperature was then raised to 100 °C and maintained for 30 min with constant stirring. Then, it was heated up to 120–130 °C and stirred for 1 h. The final composite solution was poured into Petri dishes and oven-dried at 60 °C for 14 h. This composite was synthesized with different percentages (v/v%) of graphene oxide (30%, 40%, 50%) and the thickness of all the membranes were consistently maintained between 0.28–0.30 mm.

2.6 Adopting banana leaves

Banana leaves (sourced from Padukka, Sri Lanka) were dried for varying durations, up to a maximum of 28 days (4 weeks), under controlled ambient conditions in a temperature-humidity chamber. These differently aged leaves were then adopted for the study.

2.7 Materials, and membrane characterizations

All samples were analyzed using a FTIR-PIKE spectrometer: Spectrum Two 950243, at Techno Solutions, Sri Lanka. The materials were characterized using an X-ray diffractometer model: smart lab SE, Cu-Kα radiation, at CAMD, Department of Chemistry, University of Colombo. The SEM analysis for materials were carried out by SEM model: ZEISS EVO 18, at the Department of Material Science, University of Moratuwa.

2.8 Permselectivity study

A double-chambered wooden apparatus, equipped with a membrane-fitting hole on its separating wall, was employed for the permselectivity study. Two chambers of the apparatus were filled with differently concentrated potassium chloride solutions (0.1 M and 0.01 M, assay 99.5%, Techno Pharmchem, India) which was separated by the specific ion selective membranes. Then, identical calomel electrodes were immersed in each chamber and the voltage difference across the membrane was measured with a multimeter.

2.9 Ion exchange capacity (IEC)

2.9.1 For cationic selective membranes. A titration method was used for the task. Dried membranes were cut into (1.00 g) small-flat pieces, and immersed in HCl (0.0025 M, 30.00 mL) respectively. After shaking the samples for 24 h at 100 rpm and room temperature, the membranes were washed with deionized water. Subsequently, the acid-form membranes were converted to sodium ion form by soaking in NaCl (1.00 M, assay 99.5%, Techno Pharmchem, India) solution for another 24 h. The released hydrogen ions were then titrated using NaOH (0.01 M, assay 98%, Sisco Research Laboratories).

2.9.2 For dried banana leaves. The spectroscopic method was employed for the process. Differently aged dried banana leaves were cut into 2 cm × 2 cm pieces, and immersed in KNO_3 (1.00 M, 20.00 mL) (99.50%, HiMedia Laboratories Pvt. Ltd) respectively. After shaking the samples for 24 h at 90 rpm and room temperature, the samples were washed with deionized water. Subsequently, the samples were soaked in NaCl (1.00 M, 20.00 mL) solution for another 24 h. Absorbance values of each sample (NaCl solution) were measured using a UV-visible spectrometer.

2.10 Water uptake study for banana leaves

Differently aged dried banana leaves were prepared in 2 cm × 2 cm pieces, with each piece weighed individually. Each piece was then placed in a vessel containing deionized water (30 mL) and shaken at 25 °C for 24 hours at 100 rpm. After shaking, the samples were removed, blotted dry, and reweighed. The difference in weight before and after immersion was recorded to assess water uptake.

2.11 Desalination test

A triple-chambered wooden apparatus equipped with membrane-fitting holes on its separating walls, was used for the test. To maintain charge neutrality, the end chambers were

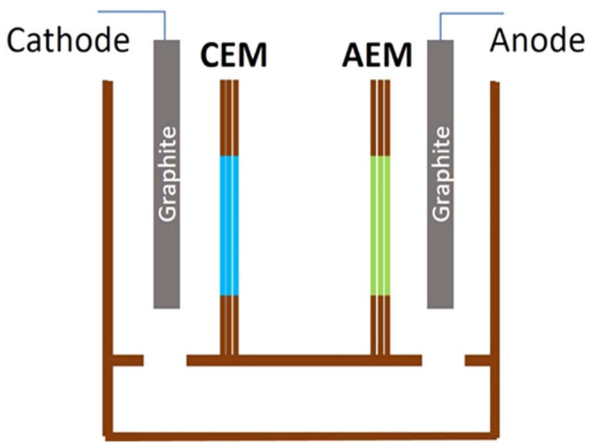

Fig. 1 Electrodialysis experimental model apparatus.

connected at their lower sections and a model diagram of the apparatus is presented in Fig. 1.

The end chambers were filled with distilled water, while the middle chamber was filled with a 3.5% (w/v) sodium chloride solution. Further, the experiment utilized the Xilong XL-666/777A Mini Pumping System, operating at a flow rate of 300 L h^{-1} as per the product specifications. The positive terminal with a carbon electrode was placed in the chamber separated by a banana leaf dried for 28 days, and the negative terminal was placed in the chamber separated by synthesized cationic selective membranes. The DC current supply was set to 30.0 V and switched on. After 20 minutes, the final conductivity of NaCl solution was recorded (at room temperature of 27 °C), and the desalination percentage was calculated using the conductivity difference.

2.12 Point zero charge analysis

The point of zero charge pH for the membranes were calculated by the pH drift method. Solutions of NaCl (0.005 M, 20 mL) was adjusted to pH 3, pH 5, pH 7, pH 9, and pH 11 separately using HCl (1.00 M) and NaOH (1.00 M). Then the membranes (0.050 g) were immersed respectively. Then the suspensions were shaken at 25 °C for 24 h at 100 rpm. After 24 h, the solution was vacuum filtered. The final pH value of the filtrate was measured. ΔpH *vs.* pHi (initial pH) was plotted to detect point zero charge of the adsorbent.

3. Results and discussion

3.1 Synthesis of carboxymethyl cellulose polymer

Cross-linking of carboxymethyl cellulose (CMC) creates, chemical bonds between polymer chains forming a three-dimensional network that resists degradation and prevents dissolution in water.[27] Citric acid (CA) reacts with hydroxyl groups of CMC to form ester bonds, while glycerol forms ether bonds with remaining hydroxyl groups. The structure of CMC and the associated reaction process between CMC and CA are depicted in Fig. 2.[28]

This cross-linked network of CMC polymer, not only improves mechanical properties and water resistance of the polymer but also introduces functional groups that facilitate cation exchange. Further, it enhances ion-exchange capacity and selectivity due to its hydrophilicity, biocompatibility, and high charge density. CMC is cost-effective compared to alternatives like alginate and chitosan, as it requires minimal modifications and provides inherent film-forming capabilities. Its compatibility with simple cross-linking techniques further reduces costs, making CMC a superior choice for efficient ion transport and challenging separations, such as Na^{+}/Mg^{2}.[11,12,29]

3.2 FT-IR analysis of CMC polymer

FT-IR analysis of synthesized CMC polymer is shown in Fig. 3. The bands between 2500–3500 cm^{-1} from the spectrum in Fig. 3 could be attributed to the carboxylic hydroxyl and intermolecular bonded hydroxyl groups of CMC. Peaks at 2932.78 cm^{-1} and 2887.48 cm^{-1} are likely due to the asymmetric stretching of

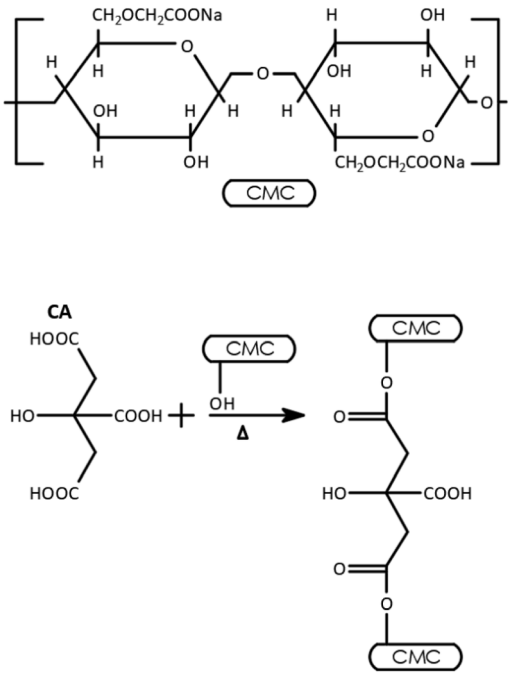

Fig. 2 Structure of CMC and cross-linking of carboxymethyl cellulose and citric acid.

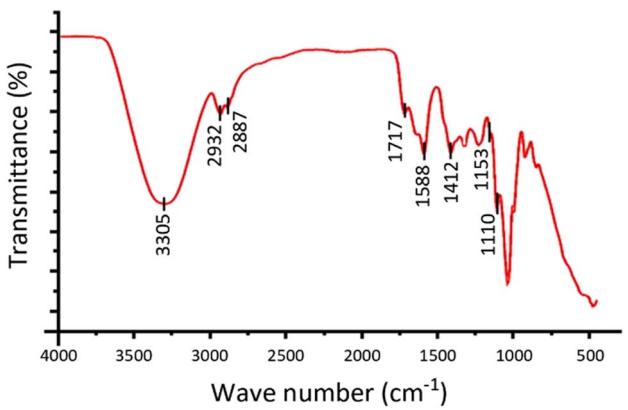

Fig. 3 FT-IR spectrum of the synthesized CMC polymer.

the $-CH_2$ groups in carboxymethyl cellulose. Typically, peaks at 1588.707 cm^{-1} and 1412.517 cm^{-1} are associated with the symmetric and asymmetric stretching of carbonyl groups.[30,31] The peak at 1717.12 cm^{-1} can be assigned to the C=O stretching of the carboxylic group, which might indicate a dimerized carbonyl stretching bond.[31]

During the cross-linking process, the formation of an ester bond is suggested by peaks at 1735–1750 cm^{-1}, though it overlaps with other peaks in this range and cannot be differentiated in this spectrum (Fig. 2). The band at 1153 cm^{-1} is likely due to aliphatic ether groups in carboxymethyl cellulose and possibly the cross-linked glycerol undergoing etherification with carboxymethyl cellulose.[32]

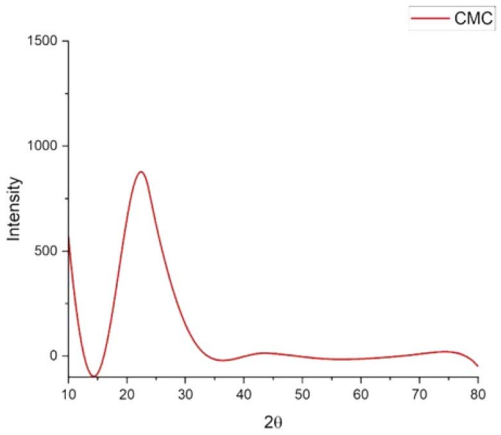

Fig. 4 XRD analysis of the synthesized CMC polymer.

3.3 X-ray diffraction analysis of CMC polymer

Characteristic peaks for CMC compound are expected to appear around 20° to 22° in XRD analysis, and the XRD patterns observed in Fig. 4 are consistent with these values,[33] confirming a successful synthesis.

3.4 Synthesis and characterization of GO

Graphene oxide (GO) was synthesized using a modified Hummers' method, which typically functionalizes graphite with a high density of oxygen-containing functional groups including hydroxyl (–OH), carbonyl, and epoxide (C–O–C), across its basal plane.[13] This modified form of GO is shown in Fig. 5,[34] and these functional groups enable GO to act as a cation-selective material, attracting positively charged ion species. Moreover, its large surface area offers a higher number of coordination sites, further enhancing its ability to facilitate cation exchange.[35]

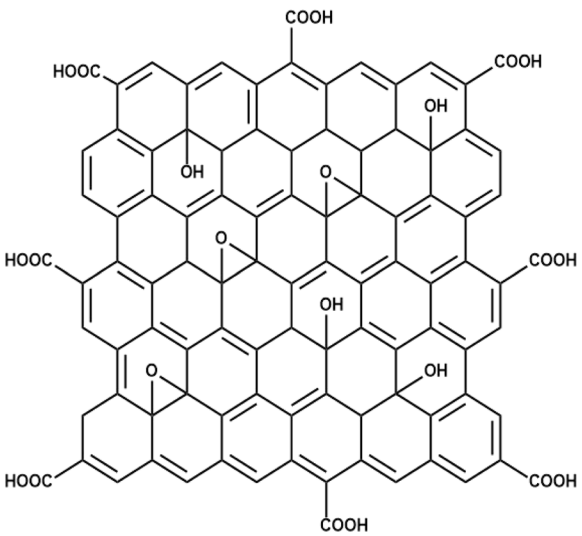

Fig. 5 Structure of synthesized graphene oxide.

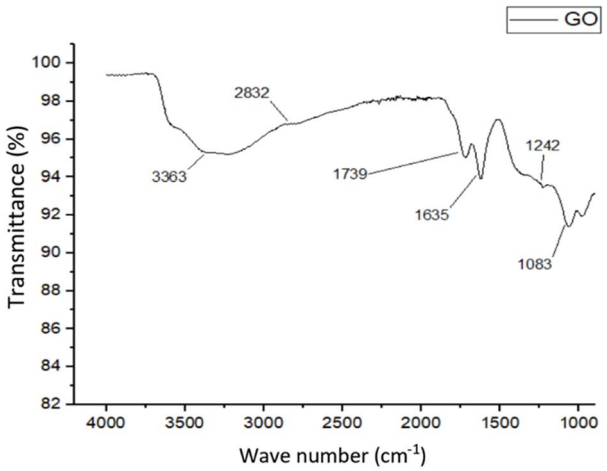

Fig. 6 FT-IR spectrum of synthesized GO by modified Hummers' method.

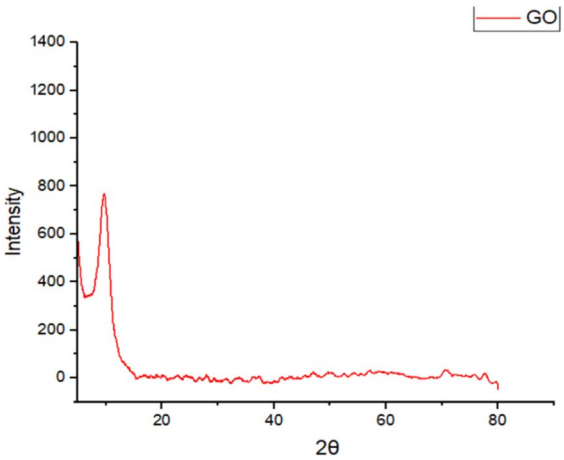

Fig. 7 XRD analysis of synthesized GO by modified Hummers' method.

3.5 FT-IR analysis of GO

According to the FT-IR analysis of GO in Fig. 6, the peaks at 3363 cm^{-1} and 2832 cm^{-1} correspond to the hydroxyl and aliphatic C–H groups in graphene oxide respectively. The peak at 1739 cm^{-1} is indicative of carboxylic vibrations, while the peak at 1635 cm^{-1} represents C=C stretching in the graphene oxide. The band at 1242 cm^{-1} can be attributed to C–O stretching of the C–OH group in graphene oxide. Additionally, the peak at 1083 cm^{-1} is related to the C–O–C band of epoxy groups.[36,37]

3.6 X-ray diffraction analysis of GO

The XRD patterns for synthesized graphene oxide illustrated in Fig. 7 align well with previously reported data,[38] validating the quality and accuracy of the synthesis. The prominent peak around 11.7° is indicative of the layered structure and interlayer spacing unique to graphene oxide.[39]

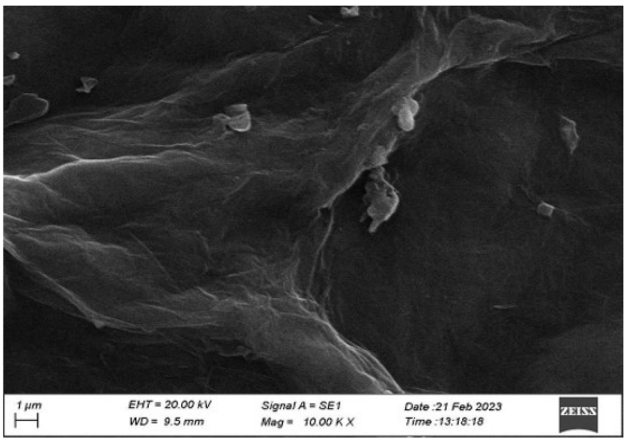

Fig. 8 SEM analysis of synthesized GO by modified Hummers' method.

3.7 SEM analysis of GO

The SEM analysis of synthesized graphene oxide is presented in Fig. 8, and it reveals a double-layer structure with a flat surface. The planar surface exhibits characteristic wrinkles, indicative of the typical morphology of GO.[37,39]

3.8 Synthesis and characterization of CMC/*Aloe vera* composite

During the synthesis, *Aloe vera* solution obtained by blending the natural gel from the leaves was mixed with CMC (as mentioned in the Experimental and methods section) prior to the cross-linking step of CMC. This approach aimed to ensure the uniform dispersion of *Aloe vera* components within the CMC polymer matrix.[31,40,41]

3.9 FT-IR analysis of CMC/*Aloe vera* composite

FT-IR spectra of *Aloe vera*, CMC polymer, and the synthesized CMC/*Aloe vera* composite are shown together in Fig. 9. It is prominent that characteristic peaks at 3435 cm^{-1} and 1642 cm^{-1} which correspond to hydroxyl groups and stretching vibrations of COO^- have intensified in CMC/*Aloe vera* composite.[30] These observations specifically indicate that the extent of anionic functional groups presents in the matrix has been enhanced with the integration of *Aloe vera* into to the CMC polymer, which is beneficial for effective cation exchange.[8,17,31]

3.10 Synthesis and characterization of CMC/GO composite

As in the previous procedure, a solution of GO was mixed with CMC before the cross-linking stage of the CMC polymer to ensure even dispersion of the synthesized GO particles across the composite.[31,35]

3.11 FT-IR analysis of CMC/GO composite

According to the obtained FT-IR spectrum for the CMC/GO composite as presented in Fig. 10(a), the peaks at 3339 cm^{-1} and 2941 cm^{-1} represent the hydroxyl and aliphatic C–H groups from both CMC and graphene oxide.[31,39] The peak at 1733 cm^{-1} corresponds to carboxylic vibration in graphene oxide.[37] Peak at 1596 cm^{-1} represent the symmetric vibration of carbonyl groups in CMC.[30,31] Overlapping peaks appearing in the FT-IR spectra in Fig. 10(b) of the CMC/GO composite could be due to the ATR mode, which detects molecular vibrational events on a shallow surface layer. The surface sensitivity of the technique gave information about interactions among carboxylate (–

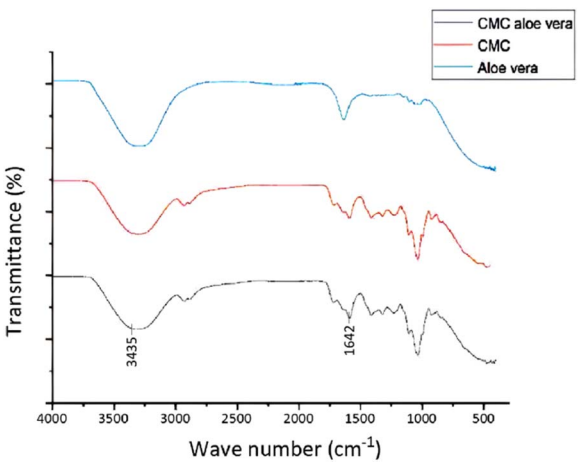

Fig. 9 FT-IR spectra of *Aloe vera*, CMC, and CMC/*Aloe vera* composite.

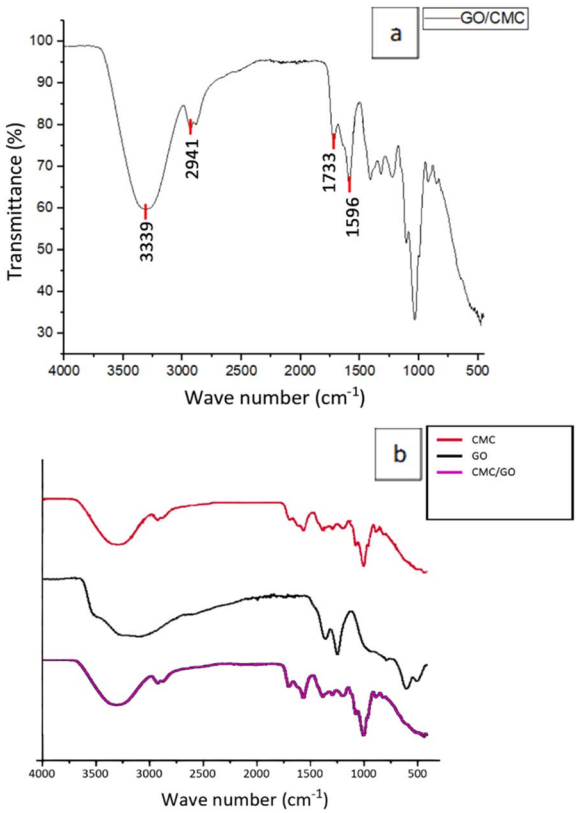

Fig. 10 FT-IR spectrum of synthesized (a) CMC/GO composite (b) CMC, GO, CMC/GO.

COO^-), hydroxyl (–OH), and carboxylic acid (–COOH) functional groups, thus leading to peaks which were broadened and overlapped by hydrogen bonding and because of the amorphous nature of the material.[16,31,37,39]

3.12 Synthesis and characterization of CMC/GO/*Aloe vera* composite

A solution of GO and *Aloe vera* was mixed together (as mentioned in Section 2) and then introduced to CMC before the cross-linked polymer formation of CMC to achieve better dispersion of GO and *Aloe vera* in the matrix.[31,35,40,41]

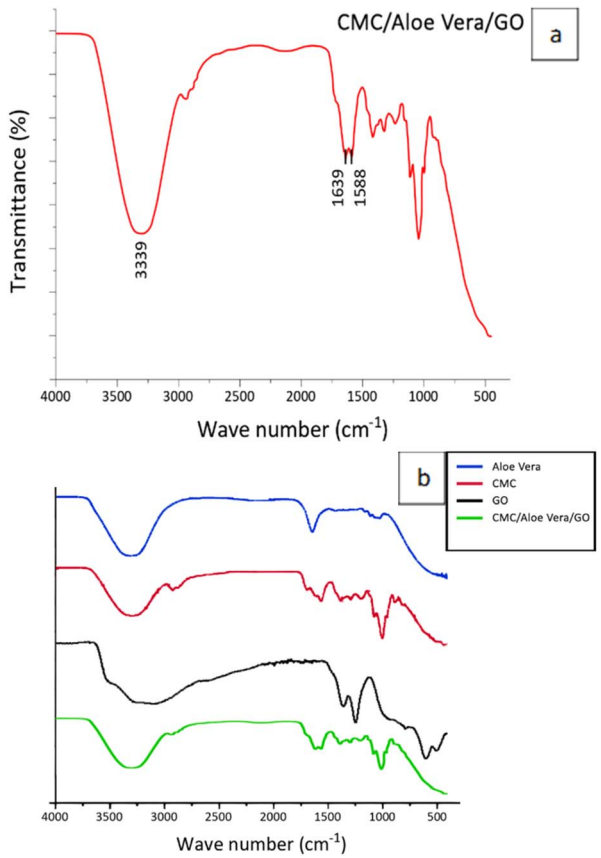

Fig. 11 FT-IR spectrum of synthesized (a) CMC/GO/*Aloe vera* composite (b) *Aloe vera*, CMC, GO, CMC/Go/*Aloe vera*.

3.13 FT-IR analysis of CMC/GO/*Aloe vera* composite

The FT-IR spectrum of CMC/GO/*Aloe vera* composite is presented in Fig. 11(a). The spectrum primarily confirms the presence of hydroxyl (3339 cm^{-1}) and carbonyl (1639 cm^{-1}, 1588 cm^{-1}) functional groups.[17,31,42] As an example, when three components are combined, the region between 1580–1735 cm^{-1} often appears overlapped (Fig. 11(b)) due to contributions from the carbonyl regions of carboxylic groups in *Aloe vera*, lateral free carboxylic ends of carboxymethyl cellulose, free carboxylic ends of graphene oxide, and the double bonds between carbon atoms in graphene oxide—all of which lie within this range.[31,42] When compared to the previous FT-IR spectra of CMC/*Aloe vera* and CMC/GO, it is evident that the combination of both components enhances the intensity of these functional groups, which is complementary for efficient cation exchange.[8,9] This observation supports the high ion exchange capacity of the composite, where the high density of carboxylate groups plays a critical role.[11,12]

3.14 Permselectivity study and ion exchange capacity study of cationic-selective composites

Experimental results of permselectivity and ion exchange capacity for each of the developed composites are tabulated in Table 1. Permselectivity refers to the selective permeability of a membrane, allowing specific ions to pass through while blocking others.[43] This is a crucial characteristic in the desalination process as it directly impacts the membrane's performance in filtering and separating desired ions.[8] According to the Table 1, the CMC/GO (50%)/*Aloe vera* composite exhibited the highest permselectivity compared to other synthesized materials. Also, there observed a prominent enhancement in permselectivity when the dosages of GO increased in the composite.[22]

Ion exchange capacity represents the total binding site for the relevant charged species within a membrane matrix.[8] The results from (Table 1), demonstrate that incorporation of GO and *Aloe vera* into the CMC polymer has significantly improved the ion exchange capacity of the membrane. This improvement can be attributed to the increased amount of cation binding sites provided by the GO and the functional group contributions from *Aloe vera* along with the porosity modifications[12,18,40,41,44] as evident from the SEM analysis (reference to Fig. 12). For comparison, Table 2 summarizes the ion exchange capacities (IEC) of several commercially available cation exchange

Table 1 The permselectivity percentages and ion exchange capacities of the developed CMC-based composites

Type of composite	Permselectivity% (percentage relative to 58 mV) ± SD	Ion exchange capacity (mmol g^{-1})
CMC	30.12 ± 0.07	0.93 ± 0.03
CMC/*Aloe vera*	39.48 ± 0.03	1.04 ± 0.06
CMC/GO	43.62 ± 0.07	1.43 ± 0.05
CMC/GO (30%)/*Aloe vera*	50.00 ± 0.11	1.47 ± 0.05
CMC/GO (40%)/*Aloe vera*	52.41 ± 0.12	1.67 ± 0.06
CMC/GO (50%)/*Aloe vera*	85.68 ± 0.15	1.88 ± 0.07

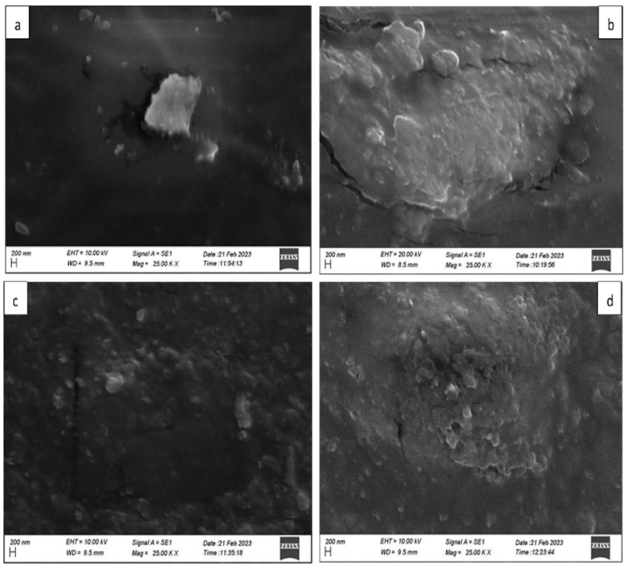

Fig. 12 SEM analysis of synthesized composites (a) CMC (b) CMC/*Aloe vera* (c) CMC/GO (d) CMC/GO (50%)/*Aloe vera*.

Table 2 Ion exchange capacities of commercially available ion exchange membranes[a]

Membrane	IEC (mmol g^{-1})
FK-40 (FuMA-Tech GmbH, Germany)	1.2–1.4
CR61-CMP (Ionics Inc., USA)	2.2–2.5
Nafion N-117 (Dupont Co., USA)	0.8–0.9
Neosepta CM-1 (Tokuyama Co., Japan)	2.0–2.5
TWCED (Tianwei Co. Ltd, China)	1.4–1.6

[a] The measurement conditions are reported by companies.[8]

membranes,[8] commonly used in applications such as electrodialysis, fuel cells, and water treatment.

According to the Table 1, developed membranes in our study have demonstrated promising IEC values, with the CMC/GO (50%)/*Aloe vera* composite showing a notable IEC of 1.88 mmol g^{-1}. This performance is competitive in contrast to commercial membranes such as FK-40 and TWCED (Table 2).[8] Overall, the synthesized membranes exhibit substantial potential for ion exchange applications, highlighting their effectiveness and viability for practical implementation.

3.15 SEM analysis of synthesized cationic-selective composites

SEM analysis of the synthesized composites of CMC, CMC/*Aloe vera*, CMC/GO, and CMC/GO/*Aloe vera* are presented in the following Fig. 12.

According to the Fig. 12(a), CMC polymer membrane exhibits a relatively smooth surface with a uniform texture and the membrane appears to have a nature of low porosity. This is likely due to the compact and tightly packed structure of the CMC polymer.[9,27,45] The CMC/*Aloe vera* composite in Fig. 12(b) displays a rougher surface with a more heterogeneous texture compared to pure CMC polymer[27,40] which can be attributed to the hydrophilic components of *Aloe vera*, such as polysaccharides and glycoproteins. Additionally, these components could significantly increase the water retention capacity of the CMC matrix, which may cause localized swelling and shrinkage during drying, leading to visible cracks and larger pores in the membrane.[12,18] Visible pores and crevices are scattered across this surface, indicating a higher level of surface irregularities, which may enhance the observed material's permeability and ion exchange capabilities.[46] The CMC/GO composite refer to the Fig. 12(c) showcases a surface characterized by both smoother and rougher areas. This variation is likely due to the presence of graphene oxide particles, which are dispersed throughout the CMC matrix in irregular shapes and a range of particle sizes, contributing to the composite's more complex surface structure.[35,44] The SEM analysis of the CMC/GO (50%)/*Aloe vera* composite in Fig. 12(d) reveals a highly porous surface with a rough texture,[35,41] where the features appear to be more uniformly distributed and smaller in size. This indicates that the integration of *Aloe vera* and graphene oxide into the CMC matrix results in a significantly porous structure that enhances ion transport and separation efficiency.[40,41,44,47] GO sheets could stabilize the structure by preventing the formation of large cracks, which would otherwise be caused by the swelling and hydrophilic interactions of *Aloe vera*. Instead, the addition of *Aloe vera* to the CMC/GO system have formed small controlled pores rather than large cracks. The functional groups of *Aloe vera*, such as carboxylic and hydroxyl groups, enhance water retention while creating small hydrated voids, without causing significant structural deformation, primarily due to the stability provided by GO.[22,40] The uniform distribution and smaller features suggest an enhanced surface area, which may contribute to improved ion transport and separation efficiency,

Table 3 The permselectivity percentages, ion exchange capacities and water uptake values of banana leaves dried for various durations[a]

Dried period of banana leaves	Permselectivity% (percentage relative to 58 mV)	Ion exchange capacity (average absorbance)	Water uptake (g) ± 0.0005 (g)
Day 1	25.16 ± 0.04	1.260	0.0322
Day 7	27.79 ± 0.05	2.023	0.0476
Day 14	47.34 ± 0.12	2.210	0.1028
Day 21	59.12 ± 0.10	2.415	0.0846
Day 28	80.17 ± 0.12	2.751	0.0586

[a] All the measurements were conducted with two trials at a temperature of 27 °C.

making the material more effective for the applications of desalination.[9,40,48,49]

3.16 Permselectivity study, ion exchange capacity and water uptake study of banana leaves

The explored parameters of permselectivity, IEC, and water uptake for banana leaves dried for various durations are presented in Table 3. The permselectivity study for the banana leaves confirmed their potential to serve as an effective anionic-selective membrane on a commercial scale. According to the results in Table 3, the permselective ability and IEC of the banana leaf improved with the increased drying period, which are essential factors for efficient desalination.[8,50]

In Table 3, the absorbance measurement for ion exchange capacity refers to the utilized spectroscopic method to calculate the IEC. An increase in the absorbance of nitrate ions suggests a higher degree of replacement by chloride ions, indicating an increase in ion exchange capacity.[51]

Ensuring minimal water absorption is essential for the effective performance of ion-selective membranes. Excessive water absorption can alter the 3-D structure of the membrane, leading to a decline in ion-exchange capacity and permselectivity by disrupting the interaction between functional groups and charged ions.[52] Further, results in Table 3 show a gradual increase in water uptake for banana leaves up to day 14, followed by a decrease. This trend suggests that modest water uptake levels in banana leaves dried for over 21 days support optimal performance, as they allow the membrane to maintain its structural integrity and selectively pass anionic species.[43] An optimum level of hydration thus aids in the well-defined development of ion-transport pathways that enhance the permselectivity along with the ion-exchange capacity.[53]

For comparison, the permselectivity of commercial anionic selective membranes typically exceeds 85%.[52] Meanwhile, banana leaves dried for 28 days demonstrated permselectivity greater than 80%, offering a greater advantage of being processed at an extremely low cost and being bio-degradable.

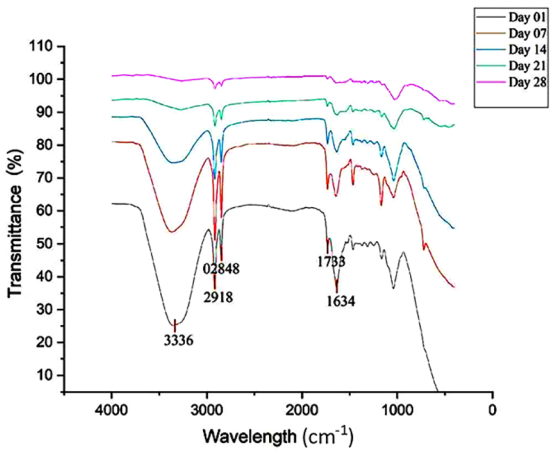

Fig. 13 FT-IR analyses of banana leaves dried for different time periods.

3.17 FT-IR analysis of dried banana leaves

FT-IR spectra of banana leaves dried for various durations are collectively shown in Fig. 13.

The FT-IR analyses of banana leaves in Fig. 13 reveals several key functional groups with distinct bands. The broad band at 3336 cm^{-1} corresponds to the hydroxyl stretching vibrations of cellulose and hemicellulose,[19] while the band at 1733 cm^{-1} is attributed to the carbonyl stretching of lignin.[54] Additionally, a band at 1634 cm^{-1} is associated with the hydroxyl stretching of water molecules.[19] Over time, the intensity of these bands decreases, suggesting the degradation of negatively charged functional groups and a reduction in water content as the banana leaves mature.[55] Also, studies[19,56,57] have indicated that C–N stretching from amine functional groups, commonly found in protein structures within the anatomy of banana leaves, typically appears around 1645 cm^{-1}. From the above FT-IR analysis in Fig. 13, this characteristic band can be observed in banana leaves dried for over 21 days, indicating the retention of amine groups during the drying process. Based on the above analysis it is suggested that dried leaves may still contain residual membrane proteins or channels within their structure,[21,58] and these components could exhibit significant selectivity for chloride ions, potentially allowing dried leaves to serve as effective anion-selective membranes.[59,60]

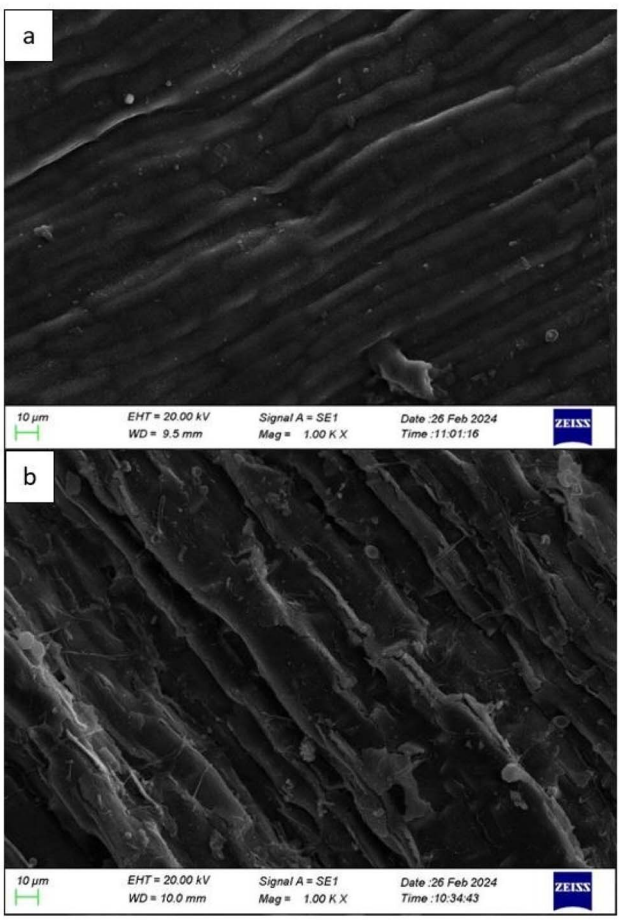

Fig. 14 SEM analysis of dried banana leaves for (a) day 1 (b) day 28.

3.18 SEM analysis of banana leaves

Obtained SEM images of banana leaves dried for 1 day and 28 days are presented in the following Fig. 14.

The SEM image of banana leaf on day 1 (Fig. 14(a)) reveals a smooth and uniform surface, with well-organized cells, indicative of an intact cutin layer.[61] However, by day 28 (Fig. 14(b)), the surface morphology undergoes a significant transformation, becoming rough, porous, and marked by discernible gaps, slits, and channels.[62] These surface irregularities are crucial as they create microenvironments that enhance adsorption by concentrating adsorbate molecules in close proximity to the surface.[62,63] This structural evolution likely contributes to the observed improvements in permselectivity and ion exchange capacity over the drying period of the leaves.[48,62] More precisely, these transformations in microstructural porosity may have facilitated the efficient passage of chloride ions through the banana leaf membrane by creating pathways that enhanced ion mobility.[53,64]

3.19 Desalination test

Desalination percentages achieved by the series of developed composites as cation exchangers, with the banana leaf dried for 28 days serving as the anion exchanger for 3.5% (w/v) [35 g L^{-1}] NaCl solutions in the apparatus are shown in Fig. 15.

According to the desalination test results shown in Fig. 15, the CMC/GO/*Aloe vera* membrane emerged as the most effective composite to serve as a cationic-selective membrane, while banana leaf dried for 28 days served as an anionic-exchanger. The CMC polymer solely achieved only about 40% desalination, while CMC/*Aloe vera*, CMC/GO composites exhibited enhanced desalination performance, consistent with the previously observed improvements in their respective permselectivity and ion exchange capacities (refer to Table 1). Notably, the CMC/GO (50%)/*Aloe vera* composite reached over 70% desalination within 20 minutes. This higher performance can be primarily attributed to the increased number of cation-binding functional sites provided by the graphene oxide and *Aloe vera* components.[17,22,35] Additionally, the morphological changes in the membrane matrix as revealed (refer to Fig. 12), potentially played a crucial role in enhancing the membrane's overall efficiency in desalination.[9,40,41,44,49]

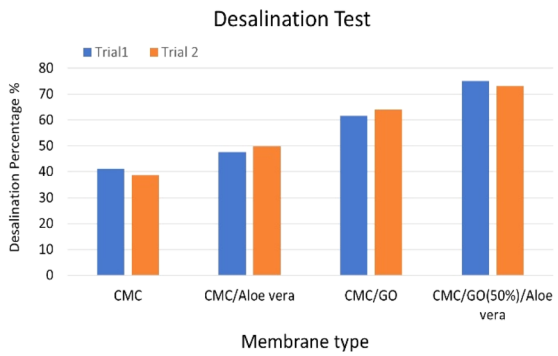

Fig. 15 Desalination percentages of 3.5% (w/v) NaCl solutions for the developed membranes as cation-exchangers and dried banana leaf as the anionic exchanger.

The performance of these membranes is particularly significant when compared to previous studies involving multi-chambered desalination systems with commercially available membranes. Those systems required more time to achieve 75% ion removal efficiency, even at lower salt concentrations (10 g L^{-1}, 5 g L^{-1}) than seawater (35 g L^{-1}), where ion removal requires less effort.[25] In contrast, our membrane system conducted desalination tests at the actual salinity level of seawater (35 g L^{-1}). Furthermore, some studies using commercially available membranes under similar seawater salinity conditions (35 g L^{-1}) unable to achieve 75% ion removal, even with multi-chambered systems and longer operation times. This demonstrates the promising energy efficiency of these bio-based ion-selective membranes in desalination.[26]

3.20 Statistical analysis

The unpaired *t*-test revealed statistically significant differences between the groups of desalination efficiencies (Table 4). The CMC/GO/*Aloe vera* composite demonstrated superior performance compared to CMC ($P = 0.0020$), CMC/*Aloe vera* ($P = 0.0031$), and CMC/GO ($P = 0.0172$). These findings further highlight the synergistic effect of incorporating both graphene oxide and *Aloe vera* into the CMC polymer matrix, resulting in a composite with enhanced properties well-suited for desalination applications.

3.21 Point zero charge analysis

The Point of Zero Charge (PZC) analysis (Fig. 16) was conducted to evaluate the membrane's performance across varying pH levels, which is crucial for determining the optimal operating conditions for desalination processes. According to the Fig. 16, the PZC value for the CMC/GO (50%)/*Aloe vera* composite was found to be approximately pH 4.5. At pH values higher than this, the membrane surface becomes negatively charged, allowing it to function as a cationic selective membrane. This occurs because the carboxylic groups in the composite release their protons as the pH exceeds 4.5, leading to the formation of a negative charge on the surface, which in turn attracts positively charged ions (cations).

Table 4 Desalination percentages of 3.5% (w/v) NaCl solutions for the developed membranes as cation-exchangers and dried banana leaf as the anionic exchanger

Type of composite	Trial number	Desalinated percentage (%)
CMC	1	41.18 ± 0.58
	2	38.67 ± 0.55
CMC/*Aloe vera*	1	47.66 ± 0.67
	2	49.89 ± 0.71
CMC/GO	1	61.63 ± 0.87
	2	64.06 ± 0.91
CMC/GO/*Aloe vera*	1	75.03 ± 1.06
	2	73.26 ± 1.04

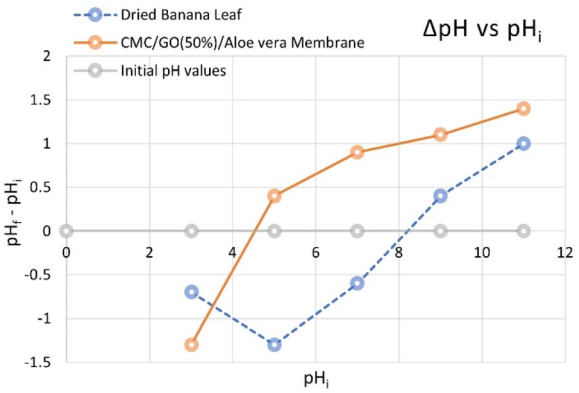

Fig. 16 Desalination percentages of 3.5% (w/v) NaCl solutions for the developed membranes as cation-exchangers and dried banana leaf as the anionic exchanger.

On the other hand, the PZC for the dried banana leaf membrane was determined to be pH 8.1. Below this pH, the surface of the banana leaf is positively charged and thus can act as an anionic selective membrane. This could be attributed to the fact that the amine groups in dried banana leaves, as revealed from the previous analysis, become protonated giving a positive charge that attracts negatively charged ions.[8,65,66]

These findings highlight the significant role of pH in controlling the ion-exchange properties of both materials. Within the pH range of 4.5 to 8.1, the CMC/GO/*Aloe vera* composite is effective as a cationic selective membrane, while the banana leaf membrane becomes suitable as an anionic selective membrane. This pH window aligns well with real-world conditions commonly encountered in natural environments, such as in lagoons, estuaries, or agricultural water supplies, where the pH typically falls within this range. As a result, the membrane system, without requiring pH pretreatment, is highly effective for desalination and can operate efficiently under these natural pH conditions, making it a practical solution for applications in environmental and agricultural water treatment systems.[50,67]

4. Conclusion

In summary, this study introduced a novel approach to desalination using electrodialysis membranes derived from natural bio-filter materials, including GO/CMC/*Aloe vera* and dried banana leaf membranes. The incorporation of graphene oxide (GO) and *Aloe vera* into the composite membranes significantly enhanced their permselectivity, ion exchange capacity, and desalination efficiency, achieving up to 75% ion removal of a 35 g per L NaCl solution (salinity of seawater). Notably, the inclusion of *Aloe vera* increased the membrane's porosity due to the properties of its bioactive compounds, which facilitated ion transport and improved overall efficiency. The GO/CMC/*Aloe vera* composite membrane exhibited superior ion exchange capacity (1.88 mmol g^{-1}), attributed to the synergistic effects of hydrophilic functional groups, with a point zero charge (PZC) of 4.5. Similarly, the dried banana leaf membranes demonstrated their potential to serve as effective anionic-selective membranes, with improved permselective ability and ion exchange capacity observed with increased drying periods. Over time, the prominence of amine groups on the surface of the dried banana leaves increased, contributing significantly to their anionic selectivity, particularly below the PZC of 8.1. These properties allow the membranes to operate efficiently in the pH range of 4.5 to 8.1, which aligns well with the natural pH of many water sources, including estuaries, lagoons, and seas. This minimizes the need for pH pretreatment. However, membranes may require optimization for extreme pH conditions, such as in highly acidic or alkaline waters (*e.g.*, salt lakes), where their performance may be compromised. Additionally, long-term performance under industrial conditions, scalability, and quantitative porosity analyses are areas for future study. The dried banana leaf membranes, while promising, may face durability challenges during scaling up due to their brittle nature, and the lifespan of the membranes under prolonged operational conditions could also be a concern. Furthermore, the hydrophilic nature of the cationic-selective membranes may promote fungal growth, requiring careful consideration in practical applications. Despite these challenges, the incorporation of GO and *Aloe vera*, along with the unique properties of dried banana leaves, has demonstrated the potential of bio-filter materials to achieve sustainable and high-performance desalination. By combining environmental sustainability, cost-effectiveness, and high efficiency, these membranes offer a promising pathway for advancing electrodialysis technology and addressing global water resource challenges.

Data availability

All data have been presented in the manuscript or in the ESI.† Any raw data can be provided on request.

Conflicts of interest

There are no conflicts to declare.

Acknowledgements

The authors would like to extend special thanks to Dr M. Shanika Fernando and Mr Manisha Gunawardana for their valuable guidance and insights on the experimental methods. We extend sincere gratitude to Mr Roshan Bandara for providing the Bogala vein graphite used in this research. We also deeply appreciate the technical officers at the Department of Chemistry, University of Colombo for their invaluable support during the laboratory sessions.

References

1 W. A. Jury and H. J. Vaux, *Adv. Agron.*, 2007, **95**, 1–76.
2 P. G. Youssef, R. K. Al-Dadah and S. M. Mahmoud, *Energy Procedia*, 2014, **61**, 2604–2607.
3 D. Song, Y. Zhang, H. Wang, L. Jiang, C. Wang, S. Wang, Z. Jiang and H. Li, *Desalination*, 2021, **507**, 115033.

4 K. Walha, R. Ben Amar, L. Firdaous, F. Quéméneur and P. Jaouen, *Desalination*, 2007, **207**, 95–106.
5 A. N. Mabrouk and H. E. S. Fath, *Desalination*, 2015, **371**, 115–125.
6 M. Bassyouni, U. Javaid and S. W. Ul Hasan, *Bio-based Hybrid Polymer Composites: A Sustainable High Performance Material*, Elsevier Ltd, 2017.
7 L. Bazinet and T. R. Geoffroy, *Membranes*, 2020, **10**, 1–72.
8 T. Xu, *J. Membr. Sci.*, 2005, **263**, 1–29.
9 R. K. Nagarale, G. S. Gohil and V. K. Shahi, *Adv. Colloid Interface Sci.*, 2006, **119**, 97–130.
10 Y. Xu, Y. Song and F. Xu, *Nano Energy*, 2021, **79**, 105468.
11 F. Xie, C. Gao and L. Avérous, *Mater. Sci. Eng., R*, 2024, **159**, 100799.
12 X. Feng and R. Pelton, *Macromolecules*, 2007, **40**, 1624–1630.
13 N. I. Zaaba, K. L. Foo, U. Hashim, S. J. Tan, W. W. Liu and C. H. Voon, *Procedia Eng.*, 2017, **184**, 469–477.
14 Y. Peng, Z. Yu, F. Li, Q. Chen, D. Yin and X. Min, *Sep. Purif. Technol.*, 2018, **200**, 130–140.
15 L. Lancellotti, A. Bianchi, A. Kovtun, M. Gazzano, T. D. Marforio, Z. Y. Xia, M. Calvaresi, M. Melucci, C. Zanardi and V. Palermo, *Nanoscale*, 2024, **16**, 7123–7133.
16 E. N. Mohamed, A. I. Abd-Elhamid, A. A. El-Bardan, H. M. A. Soliman and M. S. Mohy-Eldin, *Sci. Rep.*, 2023, **13**, 1–18.
17 N. G. Yoruk and Ö. Istanbullu Paksoy, *Food Chem.:X*, 2024, **23**, 101536.
18 G. D. Sierra-García, R. Castro-Ríos, A. González-Horta, J. Lara-Arias and A. Chávez-Montes, *Nat. Prod. Commun.*, 2014, **9**, 1217–1221.
19 S. Akbari, N. H. Abdurahman, R. M. Yunus, A. H. A. Alsaggaf and N. Ahmed, *S. Afr. J. Bot.*, 2021, **139**, 362–373.
20 S. Simal, C. Rossello, A. Femenia and E. Sánchez, *Carbohydr. Polym.*, 1999, **39**, 109–117.
21 K. Karpagavalli, I. Nithyamala, M. Srisakthilogisha, G. Nivetha, K. Thirugnanam, V. Harishanbuselvan and S. Dinesh, *J. Surv. Fish. Sci.*, 2023, **10**, 3512–3517.
22 K. H. Thebo, X. Qian, Q. Zhang, L. Chen, H. M. Cheng and W. Ren, *Nat. Commun.*, 2018, **9**, 1–8.
23 P. B. Kane, A. Contractor, S. Barwar and R. D. Kale, *Indian J. Chem. Technol.*, 2020, **27**, 243–247.
24 O. Shapira, S. Khadka, Y. Israeli, U. Shani and A. Schwartz, *Plant, Cell Environ.*, 2009, **32**, 476–485.
25 L. J. Banasiak, T. W. Kruttschnitt and A. I. Schäfer, *Desalination*, 2007, **205**, 38–46.
26 J. Shi, L. Gong, T. Zhang and S. Sun, *Membranes*, 2022, **12**, 1–11.
27 N. S. V. Capanema, A. A. P. Mansur, H. S. Mansur, A. C. de Jesus, S. M. Carvalho, P. Chagas and L. C. de Oliveira, *Environ. Technol.*, 2018, **39**, 2856–2872.
28 M. M. A. Khan, N. Rafiuddin and S. Inamuddin, *J. Ind. Eng. Chem.*, 2012, **18**, 1391–1397.
29 X. Sun, J. Shen, D. Yu and X. kun Ouyang, *Int. J. Biol. Macromol.*, 2019, **127**, 594–605.
30 A. Hivechi, S. H. Bahrami, M. Arami and A. Karimi, *Carbohydr. Polym.*, 2015, **134**, 278–284.
31 N. Habibi, *Spectrochim. Acta, Part A*, 2014, **131**, 55–58.
32 F. W. Langkilde and A. Svantesson, *J. Pharm. Biomed. Anal.*, 1995, **13**, 409–414.
33 V. Arjunan, N. Puviarasan, S. Mohan and P. Murugesan, *Spectrochim. Acta, Part A*, 2007, **67**, 1290–1296.
34 K. Gerani, H. R. Mortaheb and B. Mokhtarani, *Polym.-Plast. Technol. Eng.*, 2017, **56**, 543–555.
35 S. Gahlot, P. P. Sharma, H. Gupta, V. Kulshrestha and P. K. Jha, *RSC Adv.*, 2014, **4**, 24662–24670.
36 T. Rattana, S. Chaiyakun, N. Witit-Anun, N. Nuntawong, P. Chindaudom, S. Oaew, C. Kedkeaw and P. Limsuwan, *Procedia Eng.*, 2012, **32**, 759–764.
37 B. Paulchamy, G. Arthi and B. D. Lignesh, *J. Nanomed. Nanotechnol.*, 2015, **6**, 1–4.
38 S. Gurunathan, J. W. Han, A. Abdal Dayem, V. Eppakayala and J. H. Kim, *Int. J. Nanomed.*, 2012, **7**, 5901–5914.
39 M. Muniyalakshmi, K. Sethuraman and D. Silambarasan, *Mater. Today: Proc.*, 2020, **21**, 408–410.
40 B. Gupta, R. Agarwal, M. Sarwar Alam and J. Biomater, *Tissue Eng.*, 2013, **3**, 503–511.
41 R. Barbosa, A. Villarreal, C. Rodriguez, H. De Leon, R. Gilkerson and K. Lozano, *Mater. Sci. Eng., C*, 2021, **124**, 112061.
42 R. Wang, D. Shou, O. Lv, Y. Kong, L. Deng and J. Shen, *Int. J. Biol. Macromol.*, 2017, **103**, 248–253.
43 X. Wang, X. Zhang, C. Wu, X. Han and C. Xu, *Chem. Eng. Res. Des.*, 2020, **158**, 24–32.
44 B. Fryczkowska, D. Biniaś, C. Ślusarczyk, J. Fabia and J. Janicki, *Desalin. Water Treat.*, 2017, **81**, 67–79.
45 Y. Seki, A. Altinisik, B. Demircioğlu and C. Tetik, *Cellulose*, 2014, **21**, 1689–1698.
46 N. Kononenko, V. Nikonenko, D. Grande, C. Larchet, L. Dammak, M. Fomenko and Y. Volfkovich, *Adv. Colloid Interface Sci.*, 2017, **246**, 196–216.
47 K. Bialik-Was, K. N. Raftopoulos and K. Pielichowski, *Materials*, 2022, **15**, 748.
48 I. Stenina, D. Golubenko, V. Nikonenko and A. Yaroslavtsev, *Int. J. Mol. Sci.*, 2020, **21**, 1–33.
49 C. Klaysom, S. H. Moon, B. P. Ladewig, G. Q. M. Lu and L. Wang, *J. Membr. Sci.*, 2011, **371**, 37–44.
50 T. Sata, *J. Membr. Sci.*, 1994, **93**, 117–135.
51 F. Karas, J. Hnát, M. Paidar, J. Schauer and K. Bouzek, *Int. J. Hydrogen Energy*, 2014, **39**, 5054–5062.
52 F. D. R. Amado, L. F. Rodrigues, M. A. S. Rodrigues, A. M. Bernardes, J. Z. Ferreira and C. A. Ferreira, *Desalination*, 2005, **186**, 199–206.
53 A. K. Pandey, A. Goswami, D. Sen, S. Mazumder and R. F. Childs, *J. Membr. Sci.*, 2003, **217**, 117–130.
54 R. H. Madail, L. A. S. Pio, R. A. L. S. Rezende, M. Pasqual and S. de O. E Silva, *Acta Sci., Agron.*, 2022, **44**, 1–8.
55 F. Rexhepi, A. Surleva, A. Hyseni, M. Bruçi and B. Kodraliu, *Acta Chem. Iasi*, 2019, **27**, 263–286.
56 P. Waweru, S. T. Mukono, P. W. Ndung'u, G. Mwithiga, C. N. Onyari, G. Muriithi and S. T. Mukono, *J. Mater. Environ. Sci.*, 2020, **10**, 255–261.
57 R. D. Kale, S. Barwar, P. Kane and L. Bhatt, *European Journal of Sciences*, 2018, 26–34.

58 Y. Lu, Y. X. Qi, H. Zhang, H. Q. Zhang, J. J. Pu and Y. X. Xie, *Genet. Mol. Res.*, 2013, **12**, 6871–6881.
59 E. N. Komkova, D. F. Stamatialis, H. Strathmann and M. Wessling, *J. Membr. Sci.*, 2004, **244**, 25–34.
60 Ö. Tekinalp, P. Zimmermann, O. S. Burheim and L. Deng, *Sep. Purif. Technol.*, 2024, **332**, 125767.
61 Y. Jiang, J. Duan, T. Jiang and Z. Yang, *Micron*, 2021, **146**, 103073.
62 R. S. Wahyudi, H. S. Huboyo, E. Sutrisno and B. Zaman, *IOP Conf. Ser. Earth Environ. Sci.*, 2022, **1098**(012063).
63 A. Gundogdu, C. Duran, H. B. Senturk, M. Soylak, M. Imamoglu and Y. Onal, *Physicochemical Characteristics of a Novel Activated Carbon Produced from Tea Industry Waste*, Elsevier B.V., 2013, vol. 104.
64 K. F. L. Hagesteijn, S. Jiang and B. P. Ladewig, *J. Mater. Sci.*, 2018, **53**, 11131–11150.
65 G. M. Geise, H. J. Cassady, D. R. Paul, B. E. Logan and M. A. Hickner, *Phys. Chem. Chem. Phys.*, 2014, **16**, 21673–21681.
66 I. Rubinstein, E. Staude and O. Kedem, *Desalination*, 1988, **69**, 101–114.
67 A. Saxena, B. P. Tripathi, M. Kumar and V. K. Shahi, *Adv. Colloid Interface Sci.*, 2009, **145**, 1–22.